Continuing a Chandra Survey of Quasar Jets

Herman L. Marshall, Jonathan M. Gelbord, J.M. (MIT Kavli Inst.), Daniel A. Schwartz (CfA), Jim Lovell (ATNF), Dave Murphy (JPL), Diana Worral, Mark Birkinshaw (U. Bristol), Eric S. Perlman (UMBC), Davis Jauncey (ATNF)

MIT Kavli Institute for Astrophysics and Space Research

We continued Chandra X-ray imaging a flux-limited sample of flat spectrum radio-emitting quasars with jet-like extended structure (see Marshall et al. 2005, ApJS, 156, 13). Out of 37 jets, 22 have been detected in short exposures with Chandra, or about 59% of the sample. The X-ray flux from a powerful jet is often interpreted as inverse Compton scattering of photons from the cosmic microwave background (CMB) by electrons in a highly relativistic jet that is nearly aligned to the line of sight (IC-CMB). In this model, we can derive the distribution of angles of the jets to the line of sight if the bulk Lorentz factors are similar from object to object. The model also predicts that the spectral index from the radio to the X-ray band, α_{rx} should vary strongly with z as the CMB is brighter in the quasar jet frames at high z. We find that high z quasar jets have the same α_{rx} as lower redshift quasar jets and marginally exclude the predicted variation. This test is made more difficult by the very broad distribution of α_{rx} at all redshifts; the FWHM of the distribution of Lx/Lr is about a factor of 10.

Some of the brightest jets have been selected for follow-up Chandra observations to get more signal in individual features.

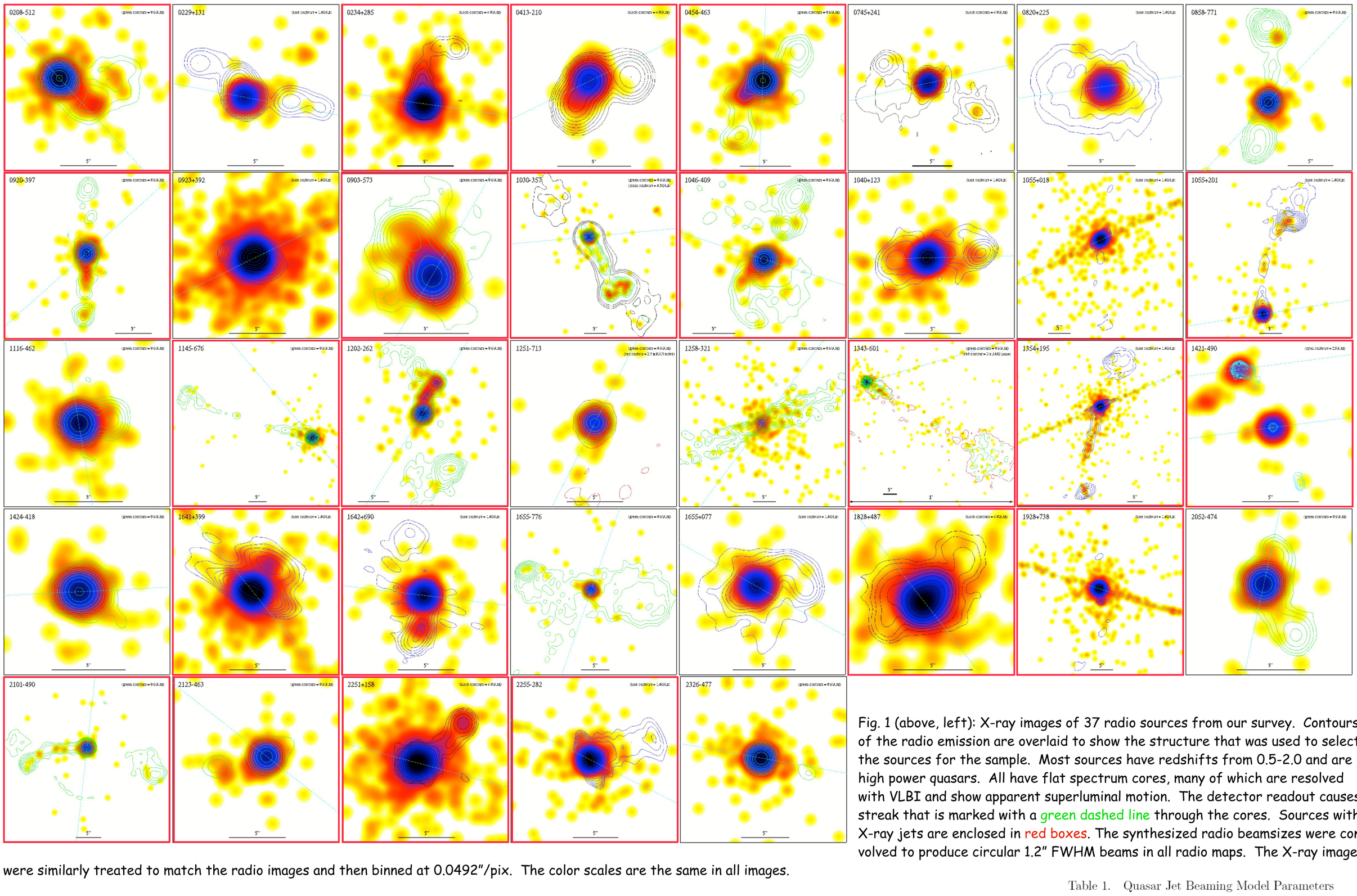

Fig. 1 (above, left): X-ray images of 37 radio sources from our survey. Contours of the radio emission are overlaid to show the structure that was used to select the sources for the sample. Most sources have redshifts from 0.5-2.0 and are high power quasars. All have flat spectrum cores, many of which are resolved with VLBI and show apparent superluminal motion. The detector readout causes a streak that is marked with a green dashed line through the cores. Sources with X-ray jets are enclosed in red boxes. The synthesized radio beamsizes were convolved to produce circular 1.2" FWHM beams in all radio maps. The X-ray images were similarly treated to match the radio images and then binned at 0.0492"/pix. The color scales are the same in all images.

Fig. 2 (left): Plot of α_{rx} against redshift. The result for PKS 0637-752 is given for comparison. The dashed line gives the dependence α_{rx} on z under the assumptions that the X-ray emission results from the IC-CMB mechanism in a relativistic jet like that of PKS 0637-752, so that the X-ray flux density would increase as $(1+z)^4$. Clearly, there is a wide distribution α_{rx}, indicating that the beaming parameters vary widely.

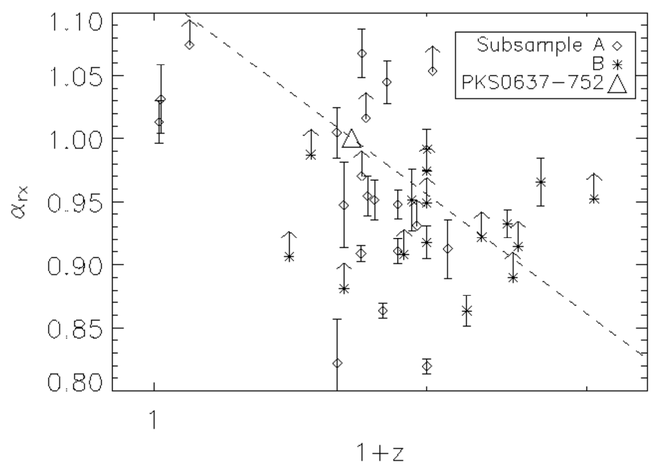

Fig. 3 (right): Distributions of α_{rx} for two different redshift groups, constructed using the Kaplan-Meier method that utilizes information in limits as well as values with small uncertainties. Under the IC-CMB model, α_{rx} should be 0.059 smaller for the high z sample. Instead, the mean α_{rx} is 0.010±0.034 larger. This marginal result could be improved with observations of the remainder of our sample.

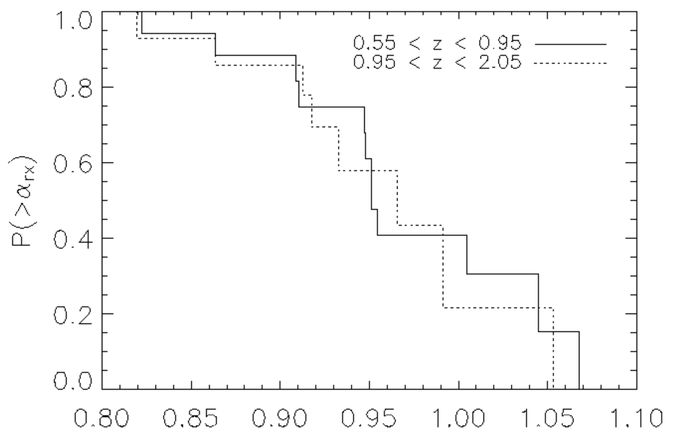

Beaming Analysis

Following Harris and Krawczynski (2002), we assume that the X-ray emission is due to inverse Compton scattering of cosmic background photons (Tavecchio et al. 2000 and Celotti et al. 2001). Marshall et al. (2005, ApJS, 156, 13) showed that the beaming parameters — the cosine of the angle θ to the line of sight μ and the jet speed β — are related to a function, K, (see Table 1) of the observables:

$$K = B_1 (a R_1)^{1/(\alpha+1)} (1+z)^{-(\alpha+3)/(\alpha+1)} b^{(1-\alpha)/(\alpha+1)}$$

by

$$K = \frac{1-\beta+\mu-\mu\beta}{(1-\mu\beta)^2}$$

where R_1 is the ratio of the X-ray and radio flux densities under the assumption that Γ = 1 (or β = 0) (see the 3rd column of Table 1) and B_1 is the minimum energy magnetic field for Γ = 1. Marshall et al. solved Eq. 1 for μ, when given Γ to give the angles in the 7th column of Table 1:

$$\mu = \frac{1-\beta+2K\beta-(1-2\beta+4K\beta+\beta^2-4K\beta^3)^{1/2}}{2K\beta^2}.$$

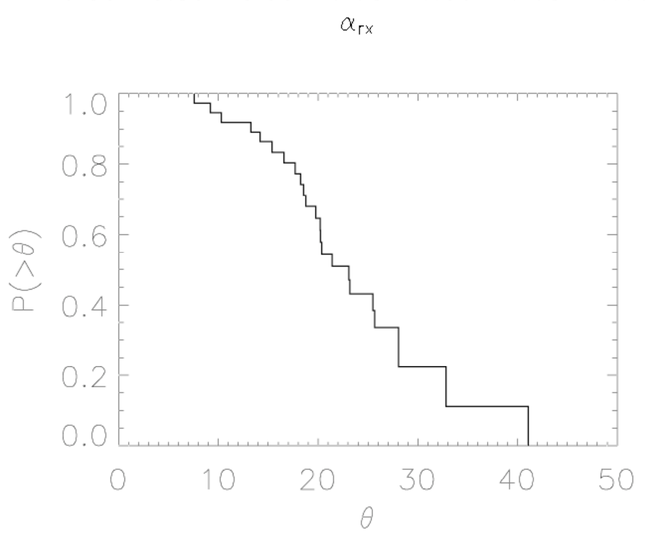

Fig. 4 (right, above): Distributions of the angle of the jet to the line of sight, θ, constructed using the Kaplan-Meier method using the data in Table 1. Randomly oriented jets would have a cos(θ) distribution where half of the sources have θ > 60°.

Table 1. Quasar Jet Beaming Model Parameters

Target	α_{rx}	R_1[a] (10^{-3})	V[b] (pc^3)	B_1[c] (μG)	K[d]	θ[e] (°)
0208−512	0.92	132.8	4.2e+15	7.4	2.34	20
0229+131	> 0.95	< 55.8	7.8e+17	1.9	< 0.15	> 40
0234+285	0.86	300.5	3.0e+16	3.4	1.34	23
0413−210	1.04	13.0	7.0e+14	17.7	1.89	21
0454−463	0.91	149.8	2.2e+15	8.2	3.23	18
0745+241	> 0.88	< 230.3	2.9e+13	11.1	< 9.88	> 13
0820+225	> 0.93	< 83.3	2.3e+15	5.4	< 1.39	> 23
0858−771	> 0.99	< 40.3	6.4e+13	14.1	< 4.25	> 17
0903−573	1.07	10.1	3.6e+14	21.5	2.28	20
0920−397	1.00	29.8	3.6e+14	13.9	3.09	18
0923+392	> 0.97	< 39.8	2.3e+14	12.5	< 2.84	> 19
1030−357	0.93	103.0	1.9e+17	3.8	0.67	28
1040+123	> 1.05	< 11.2	5.7e+15	9.6	< 0.74	> 27
1046−409	0.95	80.0	2.0e+14	10.4	3.84	17
1055+018	> 0.91	< 129.3	1.0e+16	4.6	< 1.62	> 22
1055+201	0.91	119.0	3.5e+16	3.5	0.92	25
1116−462	> 1.02	< 24.5	2.6e+14	15.8	< 2.68	> 19
1145−676	> 0.95	< 77.7	3.6e+16	4.3	< 1.01	> 25
1202−262	0.86	335.5	1.3e+15	9.5	6.32	15
1251−713	> 0.97	< 50.3	7.9e+15	5.6	< 1.02	> 25
1258−321	1.03	18.9	4.2e+08	75.6	33.47	9
1343−601	1.01	25.8	9.1e+07	106.9	56.70	7
1354+195	0.95	64.8	2.1e+15	7.6	2.21	20
1421−490	0.82	725.1	1.2e+16	5.7	4.57	17
1424−418	> 0.91	< 140.6	5.4e+16	4.7	< 0.92	> 25
1641+399	0.82	658.6	1.6e+14	6.4	7.90	14
1642+690	0.95	56.8	8.0e+14	9.3	2.40	20
1655+077	> 0.93	< 94.7	1.6e+14	9.6	< 3.87	> 17
1655−776	> 1.07	< 9.1	9.5e+10	56.6	< 14.25	> 12
1828+487	0.91	145.3	1.3e+14	22.5	10.55	13
1928+738	0.77	1785.3	1.7e+13	6.9	22.58	10
2052−474	> 0.89	< 214.4	3.8e+16	3.4	< 0.88	> 26
2101−490	0.99	37.6	1.4e+16	6.1	0.95	25
2123−463	0.97	58.4	1.9e+17	3.2	0.34	33
2251+158	0.95	72.9	1.9e+15	12.3	3.23	18
2255−282	0.95	68.5	4.2e+15	5.6	1.32	23
2326−477	> 0.92	< 123.9	3.1e+16	3.5	< 0.78	> 27

[a] R_1 is the ratio of the X-ray to radio luminosities.

[b] V is the volume of the synchrotron emission region.

[c] B_1 is the minimum energy magnetic field.

[d] K is a function of observable and assumed quantities given by eq. 1.

[e] The bulk Lorentz factor is assumed to be 10. This assumption would not be appropriate for 1343−601 because the extended material is not likely to be relativistic.

This work was supported in part by U.S. Dept. of Energy under contract No. DE-AC02-76CH03000, Smithsonian Astrophysical Observatory (SAO) contract SVI-73016 for the Chandra X-Ray Center (CXC), and NASA contract NAS8-39073.